Energy Equip. Sys./ Vol. 6/No. 3/Sep. 2018/ 247-259

ENERGY EQUIPSYS

Energy Equipment and Systems

http://energyequipsys.ut.ac.ir
www.energyequipsys.com

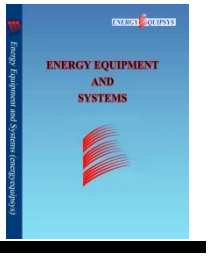

Shape optimization of impingement and film cooling holes on a flat plate using a feedforward ANN and GA

Author

Seyed Morteza Mousavi [a]
Seyed Mohammadali Rahnama [b*]

[a] School of Mechanical Engineering, College of Engineering, University of Tehran, Tehran, Iran

[b] School of Mechatronic Systems Engineering, Simon Fraser University, Vancouver, Canada

Article history:

Received : 27 December 2017
Accepted : 28 May 2018

ABSTRACT

Numerical simulations of a three-dimensional model of impingement and film cooling on a flat plate are presented and validated with the available experimental data. Four different turbulence models were utilized for simulation, in which SST $\kappa - \omega$ had the highest precision, resulting in less than 4% maximum error in temperature estimation. A simplified geometry with periodic boundary conditions is designed, based on the main geometry, and is used for the optimization procedure. Six geometrical parameters related to impingement and film holes are selected as design variables. To further reduce the time required for optimization, a feedforward neural network is implemented for the function estimation, and 584 CFD observations were performed for randomly generated design points. The data from CFD simulations were fed to network for training and test operations, and the results with good consistency were extracted from the network. The objective of the optimization is to minimize the coolant mass flow rate, subject to maximum temperature and maximum temperature gradient in solid domain being equal to or lower than their values in base design. A genetic algorithm (GA) with 100 population and 50 iterations, coupled with an artificial neural network (ANN), was used for optimization. Finally, the optimum design is simulated numerically to find the exact values of the output parameters. The CFD results for optimum design shows 44% less coolant mass flow rate while both optimization constraints are satisfied. Such a reduction in the coolant flow rate has a huge impact on the overall performance of a typical gas turbine, which is discussed in this paper.

Keywords: CFD, Impingement Cooling, Film Cooling, Gas Turbine Cooling, Optimization.

1. Introduction

The efficiency and power output of a gas turbine can be enhanced by increasing the turbine inlet temperature (TIT). This temperature is limited by the material's maximum allowable temperature. The challenge for many researchers is to find a way to surpass this limit. Apart from using a more durable material, such as thermal barrier coatings (TBC), different cooling methods described by Han et al. [1] can be implemented to increase the TIT above the allowable temperature of materials. In modern gas turbines, the combined impingement and film cooling method is a popular technique to

* Corresponding author: Seyed Mohammadali Rahnama
School of Mechatronic Systems Engineering, Simon Fraser University, Vancouver, Canada
Email: smrahnam@sfu.ca

protect the turbine blades from high temperatures of mainstream flow.

Impingement cooling is an effective way to increase the heat transfer rate between blade and coolant flow in a blade's internal passages. Martin [2] presented a review of general applications of impingement cooling. Han and Goldstein [3] reviewed the effects of different geometry and flow parameters on impingement cooling of a gas turbine system. Tabakoff and Clevenger [4] studied the effects of different jet impingement configurations on a model of blade leading edge. Metzger et al. [5] conducted an experiment to find out the effects of leading edge sharpness on impingement cooling performance. Bunker and Metzger [6] later designed and performed an experiment to measure internal heat transfer characteristics in a model of a turbine blade with impingement cooling. Owing to the complexity of geometry and flow in a real model of gas turbine blades, many researchers performed experiments on impingement cooling of flat plates [7]–[10] and studied the effects of different geometrical and flow parameters. In recent years, the CFD modeling has been used by different researchers to investigate further details of impingement cooling. Singh et al. [11] simulated an impingement cooling on a cylindrical plane and validated the results with their own experimental data. Zhao et al. [12] and Ali et al. [13] simulated the flow and heat transfer of a jet impingement over a curved surface and studied the effects of guide wall and jet to wall distance on cooling performance.

Goldstein [14] described the film cooling as the introduction of a secondary fluid into the boundary layer of a surface, to be protected from the hot mainstream flow, and reviewed the previous works in this field. Later, Goldstein et al. [15] investigated the effects of hole geometry and density on film cooling effectiveness. Sinha et al. [16] studied the local film cooling effectiveness downstream of a single row of holes. They reported that density and momentum ratios of coolant to mainstream have a significant impact on the attachment of the film layer to the surface on a flat plate. They observed the reduced effectiveness of film cooling by decreasing the density ratio and increasing the momentum ratio. Ito et al. [15] experimentally investigated the application of film cooling on a gas turbine blade and studied the effects of surface curvature on film cooling effectiveness. More recently, Yao et al. [17], [18] calculated the effectiveness of film cooling on the suction side of a turbine blade experimentally and numerically. Two review papers, presented by Bogard and Thole [19] and Bunker [20], explained the details of different parameters and their effects on film cooling of gas turbines.

Some investigations are conducted on the applications of combined impingement and film cooling. However, most researchers tend to use a flat plate instead of a blade model because of the complexity of the real blade's geometry and fluid flow. Ekkad et al. [21] presented the details of heat transfer characteristics for an array of impingement jets and a staggered array of film holes on a flat target plate. Several other researchers [22]–[25] performed similar experiments on combined impingement and film cooling with different configurations. Panda et al. [26] studied the same cooling method on a flat plate experimentally and numerically, and presented the details of geometry and boundary conditions in their experiments. Hence, their geometry is used as a base design in this research.

Three-dimensional modeling of combined impingement and film cooling with conjugate heat transfer is a time-consuming process. Hence, most researchers are intended to conduct research on a simplified two-dimensional model. Nowak et al. [27]–[30], Wang et al. [31], and Mazaheri et al. [32], all performed optimization on a simplified two-dimensional model of internal cooling of a NASA C3X blade. They utilized different objective functions to be minimized over the blade, i.e., average temperature, maximum temperature, maximum temperature gradient, and a combination of the latter two functions. More recently, Mousavi et al. [33] presented a new concept for blade cooling optimization, which is also used in this paper.

Among all the reviewed papers, we could not find a research in which the author optimizes the shape of the three-dimensional model of cooling holes in order to minimize the coolant required to keep the flat plate in a certain thermal condition. In this paper, the combined impingement and film cooling on a flat plate is simulated and the results are validated with the available experimental data. A simplified three-dimensional geometry with periodic boundary conditions is then presented to reduce the calculation time of each

observation in the optimization procedure. The optimization objective is to minimize the coolant mass flow rate with two constraints on maximum temperature and maximum temperature gradient on the flat plate. To further reduce the calculation time, a feed-forward (FF) artificial neural network (ANN) is trained by data acquired from 584 CFD observations. This network is used to predict the values of interest in other design points. A genetic algorithm (GA) is used to detect the optimum design for periodic geometry and, finally, the optimum design is simulated by CFD to calculate the exact heat transfer and flow characteristics.

Nomenclature

y^+	non-dimensional wall distance
$\dot{m}$	mass flow rate(kg/s)
Re	Reynolds number
h	Conductive heat transfer coefficient (w/m^2.K)
k	thermal conductivity (w/m.K)
V	Velocity magnitude (m/s)
P	Pressure (Pa)
T	Temperature (K)
$\hat{n}$	Surface normal direction
D	Film cooling hole diameter in base design (m)
A	Maximum allowable temperature gradient (K/m)
B	Maximum allowable temperature (K)
L	Impingement jet nozzle height from the target surface (m)
θ	Angle between film hole and impingement hole directions (degree)

Greek Symbols

ν	kinematic viscosity (m^2/s)
μ	dynamic viscosity (kg/m.s)
ρ	density (kg/m^3)

Subscripts

i	inlet
o	outlet
m	mainstream
c	coolant
tot	total
sta	static
st	steel
air	air

Abbreviations

CFD	Computational Fluid Dynamics
TBC	Thermal Barrier Coating
TIT	Turbine Inlet Temperature
RANS	Reynolds-averaged Navier-Stokes
FF	Feedforward
ANN	Artificial Neural Network
GA	Genetic Algorithm

2. Modeling

2.1. The Geometry

The geometry from Panda et al. [26] is recreated, and used as a base design to be optimized later. This geometry, which is shown in Fig.1, has a rectangular duct for hot mainstream flow across a flat steel plate with thermal conductivity of $k_{st} = 14.9\, w/m.K$. The coolant air flows through an array of impingement and film cooling holes and enters the mainstream after cooling the target plate.

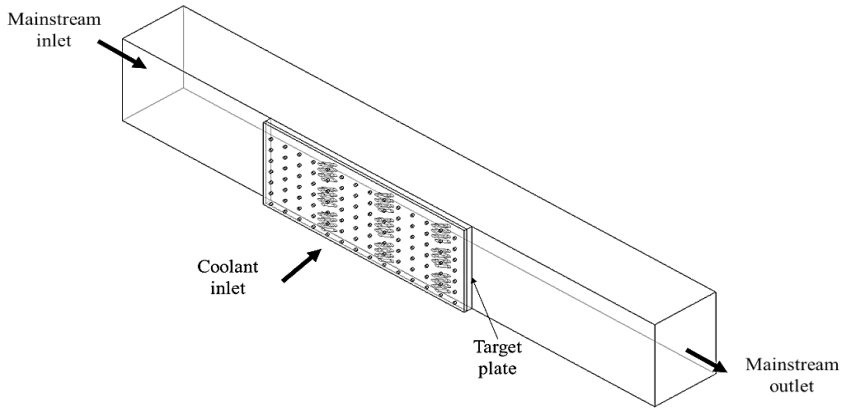

Fig.1. Base geometry of impingement and film cooling on flat plate

Modeling of the flow and heat transfer in the base geometry is very time-consuming, and it is used only to validate the numerical method. By inserting some periodic boundary conditions, a simplified geometry inspired by the base geometry is designed and used for the optimization process. By repeating the pattern of cooling holes in the periodic geometry, a geometry very similar to the base design will be generated This new simplified periodic geometry is depicted in Fig.2. Hence, all side surfaces (flat surfaces parallel to coolant inlet direction), except the mainstream inlet and outlet, will be simulated using a periodic boundary condition.

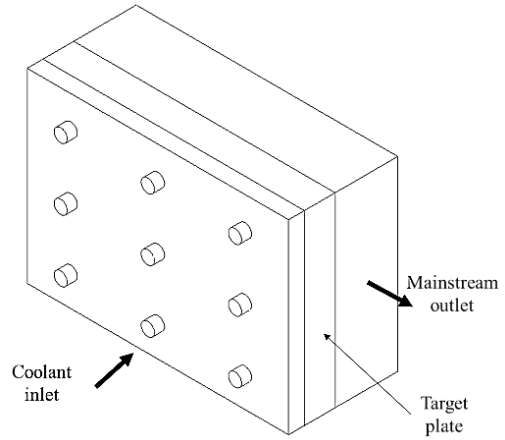

Fig.2. The simplified periodic geometry

The dimensions of the periodic geometry and the configuration of the impingement and film cooling holes are displayed in Fig.3.

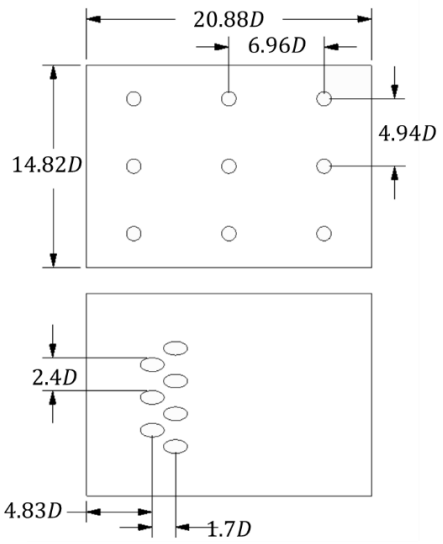

Fig.3. Impingement and film cooling holes configuration on first periodic design

The diameters of the film and impingement holes are 5 and 5.25mm respectively. The thickness of steel plate is 12.3mm and the jet nozzles have 6.3mm distance from the back side of this plate. However, some of these dimensions are design variables and will be changed during the optimization process.

2.2.Governing equations

The continuity, momentum, and energy equations should be solved simultaneously to find the field variables in this problem. The flow is assumed to be turbulence, steady state, and incompressible, and the effects of gravity and radiative heat transfer are neglected. With these assumptions, the continuity equation, the Reynolds-averaged Navier-Stokes (RANS) equations, and the energy equation can be expressed in indicial form as:

$$\text{Continuity Eq. : } \frac{\partial u_i}{\partial x_i} = 0 \tag{1}$$

$$\text{Momentum Eq. : } \rho \frac{\partial}{\partial x_j}\left(u_i u_j\right) = -\frac{\partial p}{\partial x_i} + \frac{\partial}{\partial x_j}\left[\mu\left(\frac{\partial u_i}{\partial x_j} + \frac{\partial u_j}{\partial x_i}\right)\right] - \rho \frac{\partial}{\partial x_j}\left(\overline{u_i' u_j'}\right) \tag{2}$$

$$\text{Energy Eq. : } \rho c_p \frac{\partial}{\partial x_j}\left(u_j T\right) = k \frac{\partial^2 T}{\partial x_j^2} - \frac{\partial}{\partial x_j}\left(\overline{u_j' T'}\right) \tag{3}$$

where u is velocity, x is the coordinate direction, and p and μ are the static pressure and the dynamic viscosity of the fluid. In both fluid and solid domains, ρ, c_p, k, and T represent density, specific heat capacity, thermal conductivity, and temperature respectively. The term $\overline{u_i' u_j'}$ in Eq.(2) and $\overline{u_j' T'}$ in Eq.(3) should be estimated by a proper turbulence model.

2.3.Boundary conditions

The boundary conditions used in base geometry for the numerical method validation are exactly the same as Panda et al.'s [26] experiment with a blowing ratio of 0.8. However, the boundary condition type and parameter values used in periodic geometry are slightly different. In periodic geometry, the mainstream inlet temperature is set at 800K—instead of 318K—to be more similar to the working conditions of a real gas turbine. Furthermore, in both inlet boundaries, total

pressure values are identified instead of velocity magnitude; hence, the pressure drop will be constant in every observation during the optimization process. However, the mass flow rates and Re will be different, in accordance with the design variables. The pressure values are set in a way to yield the blowing ratio of 0.8 for the first periodic geometry. The details of boundary conditions used for periodic geometry are presented in Table 1.

2.4.Optimization

In most previous works, the researchers minimize the maximum temperature or maximum temperature gradient across a blade in order to enhance the power output of the turbine. However, another parameter that has a direct effect on turbine performance is the coolant mass flow rate. According to [34], each percent of air extracted from the compressor for cooling purposes will result in a two percent loss in output power. In this research, the optimization objective is to minimize the coolant mass flow rate, with two constraints on maximum temperature and maximum temperature gradient. The objective function and two constraints for the solid domain can be expressed as:

$$Minimize: \dot{m}_c \qquad Subject\ To: \begin{cases} \max(|\nabla T|) \le A \\ \max(T) \le B \end{cases} \tag{4}$$

where A and B are respectively the maximum allowable values for temperature gradient and temperature of the solid domain. In order to achieve the same or higher reliability and lifetime for the solid part, A and B are calculated from the simulation results of the base periodic geometry.

A single objective Genetic Algorithm (GA) is utilized to solve this optimization problem. The GA is an evolutionary algorithm inspired by the process of natural selection, which is applicable for solving both constrained and unconstrained optimization problems. In this method, a population of random solutions for the optimization problem evolves to the optimum solution by means of bio-inspired operations like cross-over, mutation, and selection. This method that is widely used in shape-optimization problems is described in depth by Mitchell [35]. The number of populations for all iterations is assumed to be 100. A 1% chance is considered for the mutation of each person and, to have the elitism, the person with the maximum fitness value in each generation is directly transferred to the next generation. A maximum of 50 generations are considered for GA, which requires a lot of observations. In order to decrease the time required for 3-D CFD simulation, a feedforward neural network is trained with values obtained from 584 CFD observations. A genetic algorithm, coupled with the results of the neural network, is used to find the optimum design of the periodic geometry.

Table 1. Boundary condition type and parameter value for parametric geometry

Location	B.C. type	Parameter value
Main inlet	Pressure inlet	$P_{tot,m,i} = 101334Pa$ $T_{m,i} = 800K$ $intensity = 1\%$
Coolant inlet	Pressure inlet	$P_{tot,c,i} = 101354Pa$ $T_{c,i} = 300K$ $intensity = 1\%$
Outlet	Pressure outlet	$P_{sta,o} = 1atm$
Side surfaces	Translational periodic	-
Coupled walls	Fluid-solid interface	$u = v = w = 0$ $k_{st}\frac{\partial T}{\partial \hat{n}} = h(T - T_\infty)$
Other walls	Adiabatic wall	$u = v = w = 0$ $\frac{\partial T}{\partial \hat{n}} = 0$

2.5.Design variables

Owing to its high computational cost, it is not possible to consider all geometrical parameters for optimization. To select the most effective design variables, a method of sensitivity analysis is required. The choice of the sensitivity analysis method is dependent on several factors like research purpose, modeling cost, and number of variables [36]. In this research, a local sensitivity analysis is performed. A local sensitivity analysis is a one-at-a-time technique, in which the effect of one parameter is analyzed on the objective function while the other parameters are kept constant.
In the first step, nine geometrical parameters related to impingement and film holes are selected for analysis. Six parameters—with the highest effect on the objective function and constraints—are selected by local sensitivity analysis. Three of the selected parameters are related to impingement and the other three are related to film holes geometry. The three parameters related to impingement hole are hole inlet radius, r_1, hole outlet radius, r_2, and the height of the jet nozzle from the target surface, L. Both r_1 and r_2 have a direct effect on mass flow rate and acceleration of the flow inside the holes. Furthermore, the height of the jet nozzle from the target surface, L, determines the jet intensity. A large value of L reduces the jet intensity while increasing the coolant mass flow rate caused by lower pressure loss. Those three parameters are depicted in Fig.4 (a). The other three parameters that are related to film holes are presented in Fig.4 (b). r_3 represents the vertical radius of film hole's elliptical section (the horizontal radius is kept constant at 5 mm) and it adjusts the coolant mass flow rate and the film layer width. The vertical distance between film cooling holes, Δy, is used to control the distribution of the film layer over the target plate. Finally, the film hole angle, θ, determines how close the film layer will be to the target plate.

3.Meshing and validation

3.1.Mesh procedure

In this research, an unstructured mesh is used for all geometries, which can be automatically generated by the ANSYS Meshing tool for different geometrical designs. Several layers of prism mesh are generated near every wall in the fluid domain to capture the details of heat transfer and fluid flow in the boundary layer. The height of the first layer is selected in such a way as to keep the y^+ values smaller than five for all elements. The results on the centerline are compared using three size of meshes with different element numbers. The centerline is defined as the horizontal line passing across the center of the middle film hole on the hot side of the target plate. The grid independence analysis is depicted in Fig.5. The results for medium mesh with 5.1 million elements are in good agreement with the fine mesh, so that the same mesh size and configurations are used for all other parts in this research. The generated mesh for periodic geometry has 0.50 million elements; it is displayed in Fig.6.

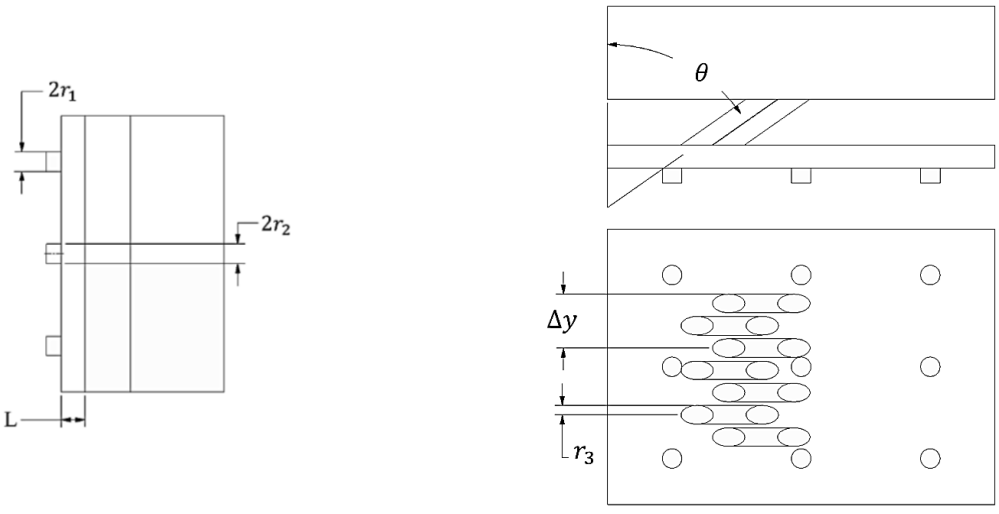

(a) (b)

Fig.4. Design variables. (a) related to impingement holes and (b) related to film holes

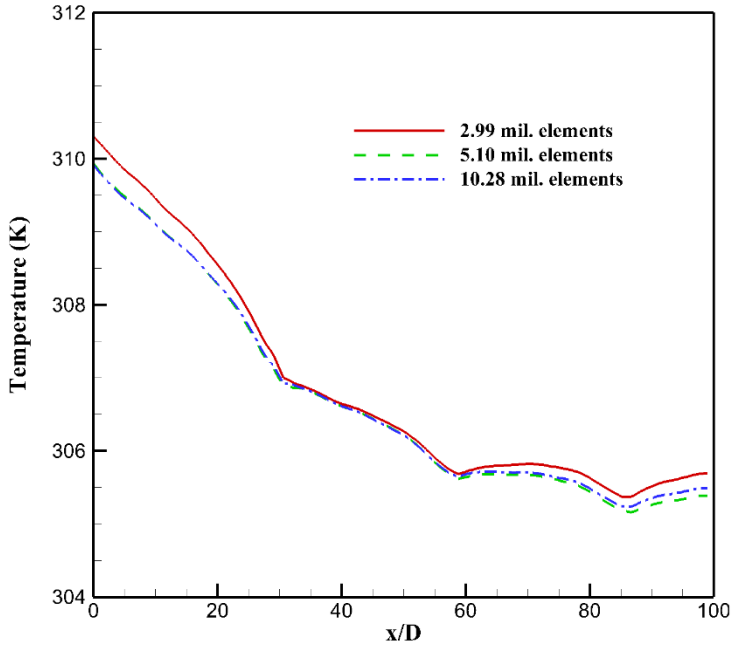

Fig. 5. Temperature on the centerline of the target surface, calculated with different mesh sizes

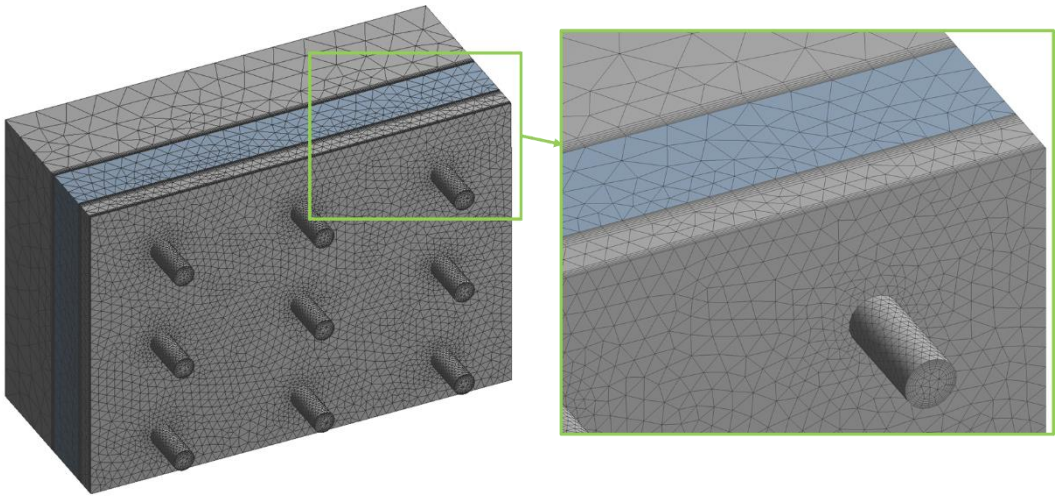

Fig. 6. Medium mesh, generated for periodic geometry

3.2.Validation

The simulation of flow and heat transfer in base geometry is conducted using ANSYS Fluent, a commercial finite volume CFD solver, with four different turbulence models, and the calculated temperature over centerline is compared with experimental data from Panda et al. [26] in Fig.7. They performed the experiments with four different blowing ratios ($M = (\rho v)_{coolant}/(\rho v)_{main}$), and used two different materials for their target plate. In this research, the CFD result of the temperature distribution on the plate's centerline is compared with experimental data for $M = 0.8$ and the steel plate. Since the y^+ is smaller than 1 in all regions, no wall function is applied to $\kappa - \epsilon$ -based turbulence models.

According to literature, the $\kappa - \epsilon$ models are generally more accurate in regions far from the walls but they perform poorly for complex flows involving severe pressure gradient, separation, and strong streamline curvature. The RNG $\kappa - \epsilon$ is usually more accurate than

normal $\kappa-\epsilon$ for rotational flows. On the other hand, the $\kappa-\omega$ turbulence model is generally more accurate for near wall regions. Shear Stress Transport (SST) is a variant of the standard $\kappa-\omega$ model, which combines the original $\kappa-\omega$ model for use near walls and the standard $\kappa-\epsilon$ model away from walls using a blending function. Furthermore, SST gives highly accurate predictions of flow separation under adverse pressure gradients, and is recommended for high accuracy boundary layer simulations, which are really important in heat transfer problems. In this case, the SST $\kappa-\omega$ is the most accurate turbulence model, which estimates the temperature with a maximum relative error of 4%.

4.Result and Discussions

4.1.Modeling of first periodic geometry

The results of the simulation for the first periodic design are used to set the constraint values in the optimization process. On the other hand, the dimensionless coolant mass flow rate of each observation is reported relative to $\dot{m}_c$ in the first periodic geometry. In each observation, the values for the coolant mass flow rate, solid maximum temperature, and solid maximum temperature gradient are calculated and used for the training of the feedforward neural network. These functions are calculated for the first periodic geometry and presented in Tabe 2.

Table 2. The results of simulation for first periodic geometry

Function	Value	Unit
$\dot{m}_{c,first}$	0.632	g/s
$\max(T)$	473.934	K
$\max(\lvert\nabla T\rvert)$	5009.6	K/m

According to the results of first periodic geometry, the A and B values in Eq. (4) are set to be $5000\ K/m$ and $480\ K$ respectively.

4.2.Neural network training

In this research, a two-layer feedforward neural network is implemented, and the activation functions of tangent-sigmoid and logarithm-sigmoid are used in the first and second layers respectively, before the output layer. The schematic of this network is depicted in Fig.8. The results of the neural network are extracted and refined in four steps, described as follows:

a. Two-layer feedforward network trained with 500 observation data and tested with the rest. We also tried one-layer and three-layer networks, but the first was not accurate enough and the latter was slower to train, without a significant impact on the results.

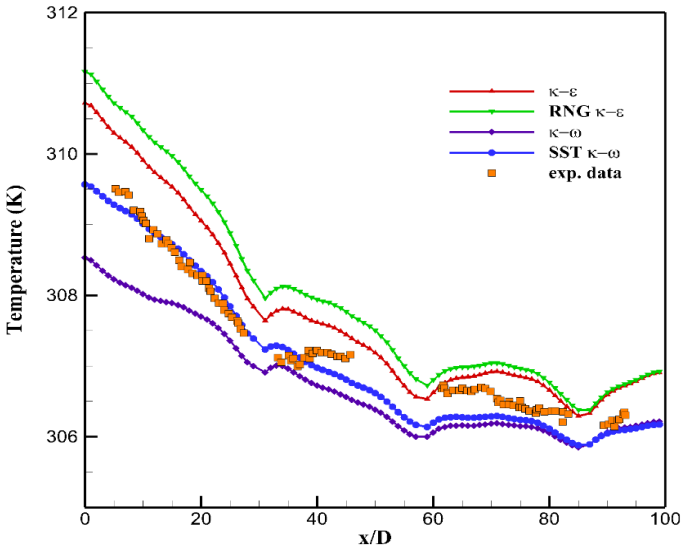

Fig.7. Validation of the numerical results with different turbulence models compared to experimental data from [26]

b. The number of neurons in each layer is optimized by trial and error to find the minimum RMS error. The network is trained by different number of neurons in first and second layers, and good accuracy and speed are observed by using 10 and 15 neurons in the first and second layers respectively.
c. Training the network (by the Levenberg–Marquardt method) is repeated five times and the average results are presented.
d. The outlier points are removed from the network input data set.

The RMS error of 0.339 was achieved by the neural network prior to applying the four steps mentioned above. This error is reduced in each step and the results became more accurate until the highly acceptable RMS error of 0.012, obtained by applying the last step. The neural network estimation of coolant mass flow rate in each of the above steps is compared with original CFD results in Fig.9. The CFD results are sorted in ascending order and the first 500 points are used for network training and later 84 points for the network test. After removing the results of 40 observations in Step 4, the train and test data counts are reduced to 490 and 54 respectively.

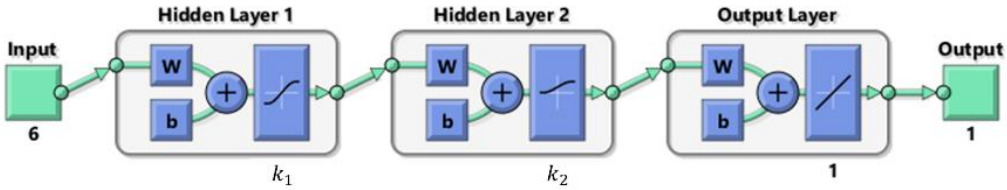

Fig.8. The schematic of feedforward neural network

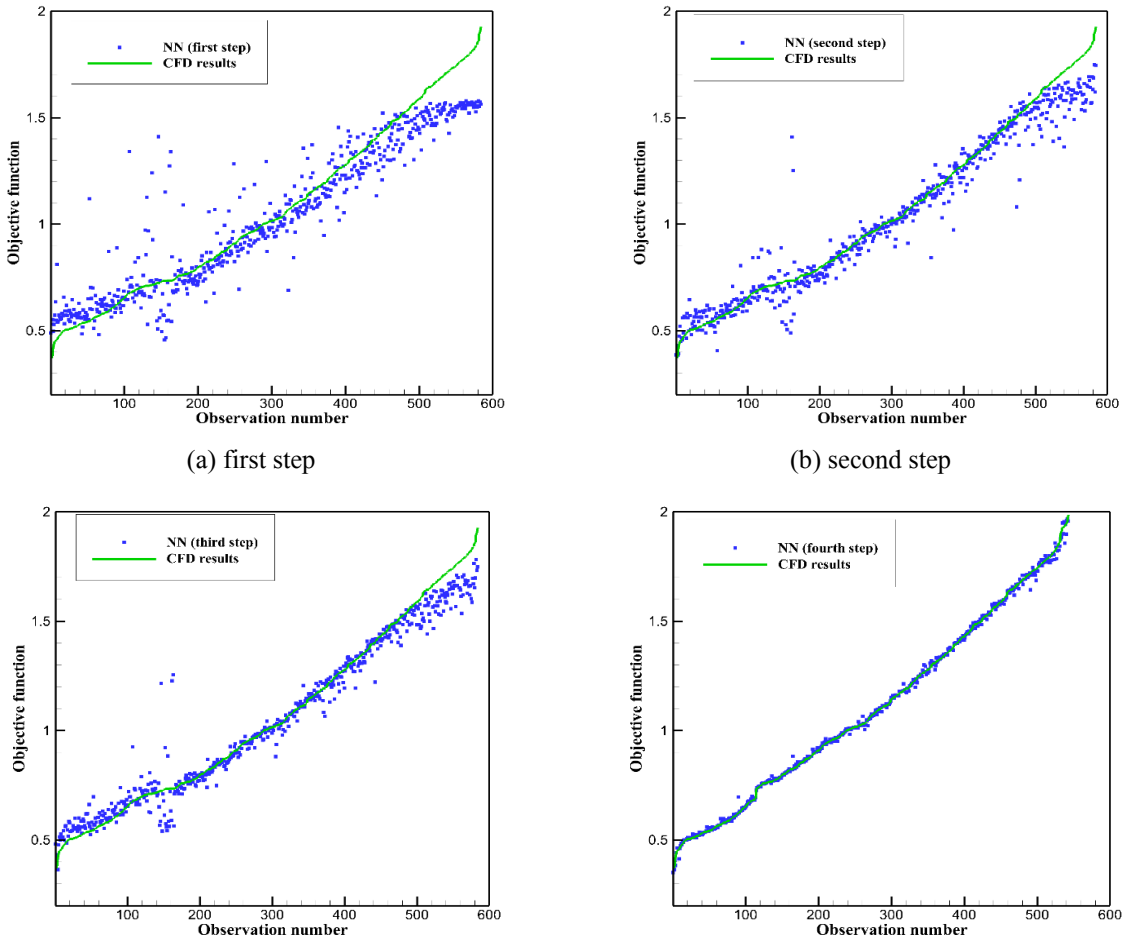

(a) first step (b) second step

(c) third step (d) fourth step

Fig.9. Comparison of the neural network results with CFD output in four steps of training

4.3.Optimization results

The genetic algorithm, with a population of 100 and maximum iterations of 50, converged to the optimum design of the cooling system with minimum coolant mass flow rate. The convergence history of GA objective function is depicted in Fig.10. The values of the design variables in optimum point are presented in Table 3.

The neural network roughly estimates the value of different functions at this point. Hence, a CFD simulation is conducted to find out the exact values. The objective function and constraint functions calculated by CFD simulation are presented in Table 3. The results show a 44% reduction in the mass flow rate required to cool the flat plate, with almost the same maximum temperature and even a lower maximum temperature gradient. A real gas turbine blade is not the topic of this research, but just to emphasize the effectiveness of coolant reduction, it should be noted that a 44% reduction in coolant mass flow rate of a typical turbine, with 15% air extraction, can lead to more than 13% enhancement of the power output.

Table 3. The optimum values for objective function and constraints calculated by CFD model

Function	Value
$\dot{m}_c/\dot{m}_{c,first}$	0.559
$\max(T)$	479.94 K
$\max(\lvert\nabla T\rvert)$	2588.1 K/m

The temperature distribution on the target plate for optimum design point is displayed by two-dimensional contours in Fig.11. It is found that the maximum temperature occurs before the film cooling holes, and the temperature of the solid plate falls after these holes. This can be explained by a view of the coolant and main flow streamlines, which are displayed in Fig.12. The coolant flow enters the mainstream through film cooling holes and creates a layer of low-temperature fluid adjacent to the solid surface and protects the surface from the hot mainstream. It is observed that in the optimum design, the inlet radius of the impingement holes, r_1, are reduced, which controls the coolant flow rate. However, the outlet radius of the impingement holes, r_2, are larger than the inlet radius in the optimum design. This means that a diverging cone shape for impingement holes might be desirable for impingement cooling, which should be studied in future works.

The fluid temperature contours are displayed on the center plane of the domain in Fig.13. The low-temperature layer of fluid, downstream of the film holes, can be recognized in this picture. By moving along the main flow direction, this layer mixes with the hot stream, and the film cooling effectiveness decreases. The optimum shape of impingement holes is also displayed in this picture, which is a diverging slot hole.

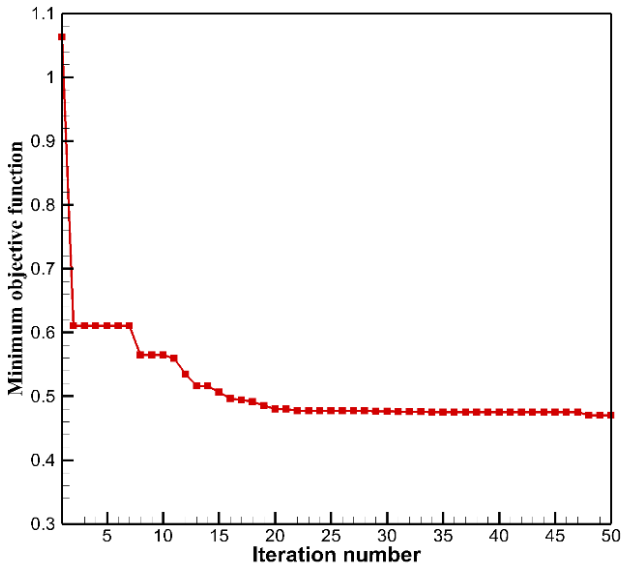

Fig. 10. Convergence history of optimization algorithm

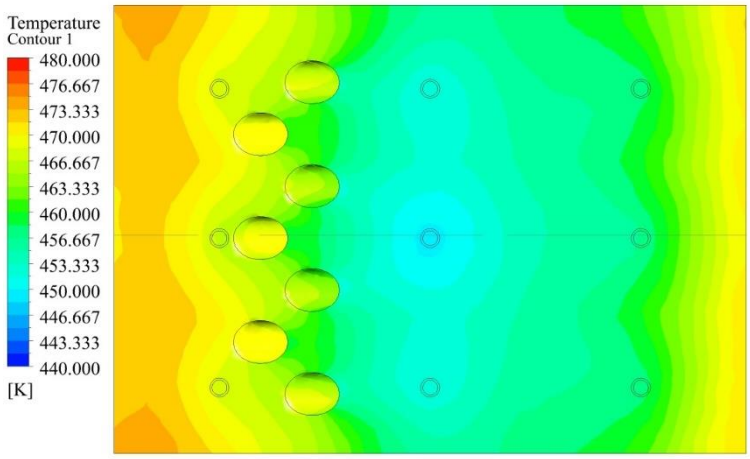

Fig.11. Temperature contours of the flat plate in optimum design point

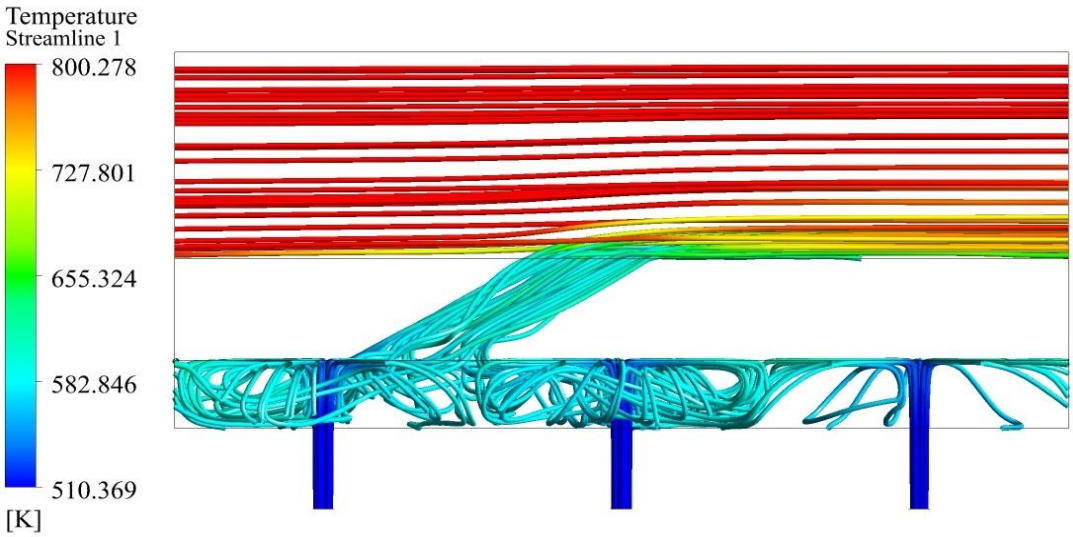

Fig.12. Three-dimensional streamlines of fluid flow, colored by temperature

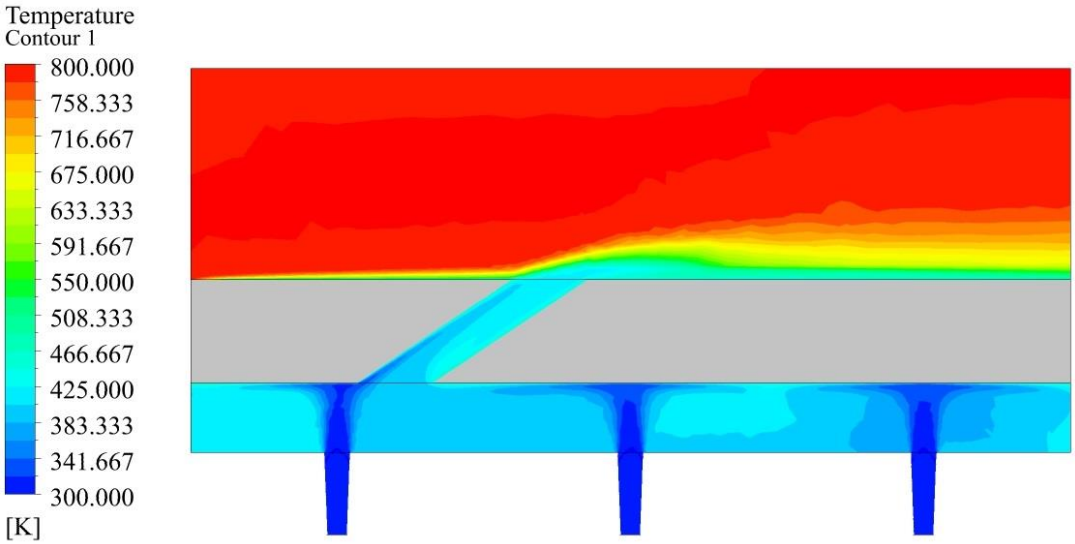

Fig.13. Temperature distribution of fluid flow on the center plane

5.Conclusion

A CFD simulation of a three-dimensional model of a flat plate with combined impingement and film is conducted and validated with available experimental data. A simplified periodic model is presented and utilized for the optimization problem. Six geometrical parameters are chosen as design variables, and 584 random design points are generated and simulated by the CFD method. A feedforward neural network is trained with the CFD results and used for the function estimation. The genetic algorithm is implemented for the optimization with the objective of mass flow rate reduction.

The shape optimization of the impingement and film cooling holes resulted in a 44% reduction in coolant mas flow rate. In case the same coolant reduction could be achieved in a real gas turbine blade, it leads to a significant increase of 13% in turbine power output of a typical gas turbine. By these means, the optimization method offered in this research may further increase the turbine output, compared to previous works in this field.

Neural networks reduced the time required for optimization procedure by more than 88% in this research. Almost 5,000 observations were estimated by neural network during the optimization process in a matter of seconds, while only 584 time-consuming CFD simulations were performed for network training.

The cylindrical impingement holes were reformed to diverging slots in the optimum design point. It is concluded that the diverging slots are able to increase the heat transfer or reduce the temperature gradient in the impingement cooling method, and should be considered for future works.

References

[1] Han J.-C., Dutta S., Ekkad S., Gas Turbine Heat Transfer and Cooling Technology, Second Edition (2012)27.

[2] Martin H., Heat and Mass Transfer between Impinging Gas Jets and Solid Surfaces, in Advances in Heat Transfer (1977)13(C):1–60.

[3] HAN B., GOLDSTEIN R. J., Jet-Impingement Heat Transfer in Gas Turbine Systems, Annals of the New York Academy of Sciences (2001) 934(1): 147–161.

[4] Tabakoff W., Clevenger W., Gas Turbine Blade Heat Transfer Augmentation by Impingement of Air Jets Having Various Configurations, Journal of Engineering (1972) 94(1):51.

[5] Metzger D. E., Baltzer R. T., Jenkins C. W., Impingement Cooling Performance in Gas Turbine Airfoils Including Effects of Leading Edge Sharpness, Journal of Engineering (1972) 94(3):219.

[6] Bunker R. S., Metzger D. E., Local Heat Transfer in Internally Cooled Turbine Airfoil Leading Edge Regions: Part I—Impingement Cooling Without Film Coolant Extraction, Journal of Turbomachinery (1990) 112(3)451.

[7] San J.-Y., Lai M.-D., Optimum Jet-to-Jet Spacing of Heat Transfer for Staggered Arrays of Impinging Air Jets, International Journal of Heat and Mass Transfer (2001) 44(21):3997–4007.

[8] Brevet P., Dejeu C., Dorignac E., Jolly M., Vullierme J. J., Heat Transfer to a Row of Impinging Jets in Consideration of Optimization, International Journal of Heat and Mass Transfer (2002) 45(20): 4191–4200.

[9] Wang T., Lin M., Bunker R. S., Flow and Heat Transfer of Confined Impingement Jets Cooling Using a 3-D Transient Liquid Crystal Scheme, International Journal of Heat and Mass Transfer (2005) 48(23–24): 4887–4903.

[10] Goodro M., Park J., Ligrani P., Fox M., Moon H.-K., Effects of Mach Number and Reynolds Number on Jet Array Impingement Heat Transfer, International Journal of Heat and Mass Transfer (2007) 50(1–2):367–380.

[11] Singh D., Premachandran B., Kohli S., Experimental and Numerical Simulation of the Jet Impingement Cooling of a Circular Cylinder, Numerical Heat Transfer Part A Applications (2013) 64(2): 153–185.

[12] Zhao Q.-Y., Chung H., Choi S. M., H. Cho H., Effect of Guide Wall on Jet Impingement Cooling in Blade Leading Edge Channel, Journal of Mechanical Science and Technology (2016) 30(2):525–531.

[13] Al Ali A. R., Janajreh I., Numerical Simulation of Turbine Blade Cooling via Jet Impingement, Energy Procedia (2015) 75:3220–3229.

[14] Goldstein R. J., Film Cooling, in Advances in Heat Transfer (1971)321–379.

[15] Ito S., Goldstein R. J., Eckert E. R. G., Film Cooling of a Gas Turbine Blade," Journal of Engineering and Power (1978) 100 (3): 476.

[16] Sinha A. K., Bogard D. G., Crawford M. E., Film-Cooling Effectiveness Downstream of a Single Row of Holes With Variable Density Ratio, Journal of Turbomachinery (1991) 113(3): 442.

[17] Yao Y., Zhang J.-Z., Wang L.-P., Film Cooling on a Gas Turbine Blade Suction Side with Converging Slot-Hole, International Journal of Thermal Sciences (2013) 65: 267–279.

[18] Yao Y., Zhang J., Tan X., Numerical Study of Film Cooling From Converging Slot-Hole on a Gas Turbine Blade Suction Side, International Communications in Heat and Mass Transfer (2014) 52: 61–72.

[19] Bogard D. G., Thole K. A., Gas Turbine Film Cooling, Journal of Propulsion and Power (2006) 22(2): 249–270.

[20] Bunker R. S., A Review of Shaped Hole Turbine Film-Cooling Technology, Journal of Heat Transfer (2005) 127(4): 441–453.

[21] Ekkad S. V, Huang Y., Han J.-C., Impingement Heat Transfer on a Target Plate with Film Cooling Holes, Journal of Thermophysics and Heat Transfer (1999) 13(4): 522–528.

[22] Oh S. H., Lee D. H., Kim K. M., Kim M. Y., Cho H. H., Enhanced Cooling Effectiveness in Full-Coverage Film Cooling System With Impingement Jets," ASME Conference Proceedings (2008) 2008 (43147): 735–744.

[23] Wang K., Li H., Zhu J., Experimental Study of Heat Transfer Characteristic on Jet Impingement Cooling with Film Extraction Flow, Applied Thermal Engineering (2014) 70(1): 620–629.

[24] Mensch A., Thole K. A., Overall Effectiveness of a Blade Endwall With Jet Impingement and Film Cooling, The Journal of Engineering Gas Turbines Power (2013)136 (3): 31901.

[25] Shi B., Li J., Li M., Ren J., Jiang H., Overall Cooling Effectiveness on a Flat Plate With Both Film Cooling and Impingement Cooling in Hot Gas Condition, in Volume 5A: Heat Transfer, (2016) V05AT10A007.

[26] Panda R. K., Prasad B. V. S. S. S., Conjugate Heat Transfer FROM a Flat Plate with Shower Head Impinging Jets, Front, Heat Mass Transfer (2012) 2(1): 1–10.

[27] Nowak G., Wróblewski W.O, Chmielniak T., Optimization of Cooling Passages Within a Turbine Vane, ASME conference proceedings (2005) 2005(47268): 519–525.

[28] Nowak G., Wróblewski W., Thermo Mechanical Optimization of Cooled Turbine Vane, in Volume 4: Turbo Expo 2007, Parts A and B (2007) 0: 931–938.

[29] Nowak G., Wróblewski W., Cooling System Optimisation of Turbine Guide Vane, Applied Thermal Engineering (2009) 29(2–3): 567–572.

[30] Nowak G., Wróblewski W., Optimization of Blade Cooling System with Use of Conjugate Heat Transfer Approach, International Journal of Thermal Sciences (2011) 50(9): 1770–1781.

[31] Wang B., Zhang W., Xie G., Xu Y., Xiao M., Multiconfiguration Shape Optimization of Internal Cooling Systems of a Turbine Guide Vane Based on Thermomechanical and Conjugate Heat Transfer Analysis, Journal of Heat Transfer (2015) 137(6): 61004.

[32] Mazaheri K., Zeinalpour M., Bokaei H. R., Turbine Blade Cooling Passages Optimization Using Reduced Conjugate Heat Transfer Methodology, Applied Thermal Engineering (2016) 103: 1228–1236.

[33] Mousavi S. M., Nejat A., Kowsary F., Optimization of Turbine Blade Cooling with the Aim of Overall Turbine Performance Enhancement, Energy Equipment and Systems (2017) 5(March): 71–83.

[34] Brooks F. J., GE Gas Turbine Performance Characteristics (2000).

[35] Mitchell M., An Introduction to Genetic Algorithms, Computers & Mathematics with Applications (1996) 32(6): 133.

[36] Tian W., A Review of Sensitivity Analysis Methods in Building Energy Analysis, Renewable and Sustainable Energy Reviews (2013) 20: 411–419.